RESEARCH PAPER

Scaling effects on flow hydrodynamics of confined microdroplets induced by Rayleigh surface acoustic wave

M. Alghane · Y. Q. Fu · B. X. Chen · Y. Li · M. P. Y. Desmulliez · A. J. Walton

Abstract This paper reports an experimental and numerical investigation on the scaling effects in the flow hydrodynamics for confined microdroplets induced by a surface acoustic wave (SAW). The characteristic parameters of the flow hydrodynamics were studied as a function of the separation height, H, between the $LiNbO_3$ substrate and a top glass plate, for various droplets volumes and radio-frequency powers. The ratio of the gap height to attenuation length of the SAW, H/l_{SAW}, is shown to be an important parameter affecting the streaming flow induced in this confined regime. The reported numerical and experimental results are in good agreement over the range examined in this study and demonstrate that, at a lower gap heights of $H \leq 100$ μm, a significant decrease in streaming velocity or Reynolds number is induced, with the velocity approaching zero when the gap height is decreased to ~ 50 μm. An increase in the gap height results in an increased streaming velocity; however, if the gap height exceeds 70 % of the SAW attenuation length, any further increase in the gap height induces a drop in the streaming velocity.

Keywords Microdroplet · Scaling · Confined · Mixing · Surface acoustic wave

M. Alghane · Y. Q. Fu (✉) · B. X. Chen (✉) ·
M. P. Y. Desmulliez
School of Engineering and Physical Sciences,
Institute of Integrated Systems, Heriot-Watt University,
Edinburgh EH14 4AS, UK
e-mail: richard.fu@uws.ac.uk

B. X. Chen
e-mail: B.Chen@hw.ac.uk

M. Alghane
Mechanical Engineering Department, Engineering College,
University of Omar Al-Mukhtar, Al Bayda, Libya

Y. Q. Fu
Thin Film Centre, Scottish Universities
Physics Alliance (SUPA), University of West of Scotland,
Paisley PA1 2BE, Scotland, UK

Y. Li · A. J. Walton
Scottish Microelectronic Centre, School of Engineering, Institute
for Integrated Systems, Institute for Integrated Micro and Nano
Systems, University of Edinburgh, Edinburgh EH9 3JF, UK

1 Introduction

Over the past 10 years, surface acoustic wave (SAW) devices have been developed extensively for microfluidic applications (Friend and Yeo 2011). A SAW-induced streaming phenomenon has been used to enhance mixing and agitation in both microdroplet (digital) and micro-channel-based microfluidic systems (Franke and Wixforth 2008). Whereas a SAW-induced streaming has been studied extensively in digital microfluidics (Wixforth 2003; Alghane et al. 2011), fewer studies have been reported for SAW microfluidics in confined spaces or microchannels (Tan et al. 2010).

In some recent work (Tan et al. 2007, 2009, 2010), a top-open microchannel was fabricated on the substrate surface of a $LiNbO_3$ SAW device using laser micromachining. These studies showed that the changes in the SAW excitation frequencies switch the flow pattern from uniform (parallel) to mixing (vortical) flow, depending on the ratio of wavelength to microchannel width. Gu et al. (2009) studied the performance of a non-contact linear motor driven by a SAW through a thin liquid layer on which the slider was suspended. The motor was contained within a top-open glass cell located at the SAW device surface.

Results showed that the velocity of the slider is proportional to the power applied to the SAW device, and is also dependant on the thickness of the liquid layer. For semi-closed microfluidic systems, Shiokawa et al. (1989a, b) reported that placing a guide plate on top of a liquid layer is an effective method to control the flow of liquid in the propagation path of SAW, but the flow velocities were slower than that of liquid without top plate, due to the resultant shear gradient induced at the surface of the top plate. A similar experimental set up has also been used in many SAW-mixing studies (Frommelt et al. 2008a, b), and results showed that the flow patterns in the droplets with a top plate enhanced the mixing efficiency of the contained microparticles. For closed microchannels, Schmid et al. (2011) observed that the scattering of SAW energy which was leaked through a liquid layer into the upper glass slide generated an acoustic power, which was able to drive and pump biological substances in a rectangular polydimethylsioxane (PDMS) microchannel located on the glass slide. SAW-induced streaming has been reported to be one of the more efficient techniques to enhance mixing efficiency in a continuous microchannel flow (Luong et al. 2011; Zeng et al. 2011).

Microchannel design (shape and geometry) has also been reported to influence the flow characteristics inside the microchannels (Kang et al. 2005). For example, microchannel height has been reported to have significant influences on the characteristic flow parameters of streaming phenomena induced by a flexural plate wave (FPW) (Nguyen and White 1999; Nam-Trung and White 2000; Tzong-Shyng and Horng-Jiann 2009). Min-Chien and Tzong-Shyng (2007) showed that, within a microchannel with a height <100 μm, the induced shear stress from the side walls causes a significant effect on the

streaming velocity profiles. Guo et al. (2008) theoretically studied the acoustic streaming generated by a lead zirconium titanate (PZT) piezoelectric ceramic plate attached to the bottom of micro-machined silicon microchannel. Their results showed that acoustic streaming velocity was dependent not only on the acoustic power but also on the channel height, and a maximum streaming velocity was increased from 0.16 to 0.2 m/s by increasing the channel height from 0.5 to 1 mm.

Clearly all these studies exhibit apparent significant scaling effects of height on the streaming flow induced by acoustic waves in confined microdroplets or microchannels. However, it should be noted that most studies of height effects induced by SAW streaming were based on the microdroplet or open microchannels with no top-plate. So far, to the best of our knowledge, there have been no systematic studies of the height scaling effect on SAW streaming in a confined microdroplet. Clearly, a simple but an efficient method is needed to evaluate this scaling effect in confined microfluidics and hence this study presents experimental and numerical investigations for the height scaling effects on the characteristic flow hydrodynamics for confined microdroplets actuated with SAW technology.

2 Experimental and numerical details

The configuration of the experimental set-up includes a glass slide and a LiNbO$_3$ substrate, the latter of which generates the SAW. The slide and substrate are separated by a distance H and a water microdroplet placed between them, as schematically illustrated in Fig. 1. The microfluidic experiments were carried out using 128° YX-LiNbO$_3$ SAW devices with an aperture of 1.5 mm, a finger width of
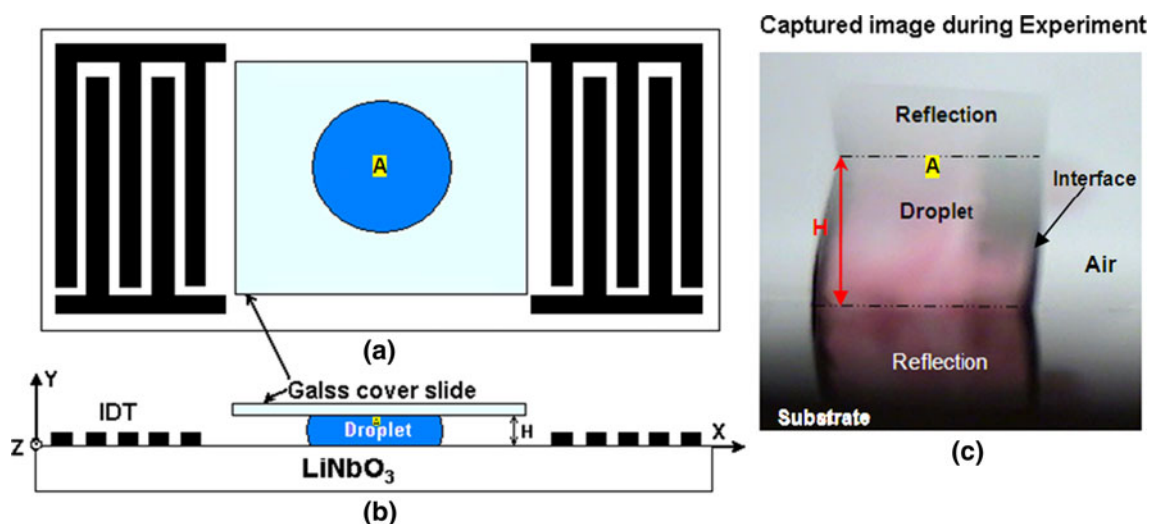

Fig. 1 Schematic illustration of experimental and numerical setups. a Top view; b cross-sectional view; c captured cross-section image of 4 μl droplet from side view during the experiment with a gap height (H) of 1,113 μm

16 μm and a wavelength of 64 μm. The measured excitation frequency of the SAW device is ∼60 MHz. In this study, a CYTOP® (Asahi Glass Co., Ltd., Tokyo Japan) layer was spin-coated on both the top glass slide and LiNbO$_3$ SAW substrate surface to make the surfaces hydrophobic, as hydrophilic surface has been reported to suppress the streaming velocity (Shiokawa et al. 1989a, b). The space between the top glass plate and substrate, defined in this article as the gap height H, were set to 65, 102, 271, 548 and 1,113 μm using specially designed spacers, and the droplet volumes were adjusted in order to maintain a constant droplet diameter of either ∼2.2 or ∼3 mm. In order to determine the streaming velocity, polystyrene particles with average diameters of 6 μm were placed inside the water droplets and their motions were recorded using a high speed camera (Kodak Motion Corder Analyzer-600 frames per second).

For the flow hydrodynamic simulations, the laminar incompressible Navier–Stokes equation of SAW-liquid coupling (Alghane et al. 2010), driven by an external body force, F, was solved numerically in three-dimension using a finite volume numerical method (Patankar 1980). The meshing of the confined droplet domain was built using a curvilinear grid structure with a grid size of $50 \times 25 \times 50$ cell nodes, in x, y and z axis, respectively. As can be observed from Fig. 1c, the interface curvature of the droplet is small and can be reasonably approximated by a straight line with a wetting angle of ∼90°. Hence in the simulation, the droplet contact angle at solid surfaces was assumed to be 90° and the small deviation from the actual contact angle was ignored. In all the experimental tests of this study, no significant deformation at the droplet/air interface was observed due to the low SAW power used during the streaming process, therefore, a slip (stress free) boundary condition on the droplet/air interface, and a non-slip boundary condition on the droplet/solid surfaces (glass slide and substrate surface) were assumed, as indicated in Fig. 1. The streaming simulations were carried out using a SAW device with an excitation frequency of 60 MHz. As mentioned above, the droplet volumes were set by fixing the droplet diameter at 2 mm with gap heights of 50, 100, 250, 333, 400, 500, 600, 750 and 1,000 μm. RF powers ranging from 0.5 to 50 mW were applied in the simulations.

3 Results and discussions

3.1 Streaming velocity versus RF power and gap height

Variations of the streaming velocity as a function of the RF power and gap height were studied both experimentally and theoretically. From the results, the streaming velocity is dependent not only on the RF power and liquid volume
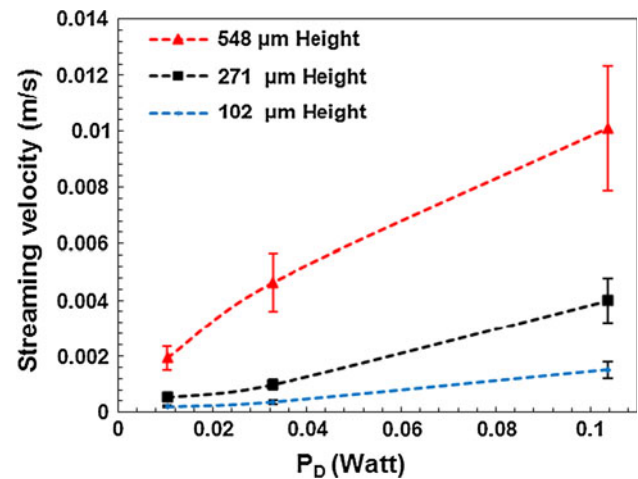

Fig. 2 Experimental measurements of maximum streaming velocity as a function of RF power for a ∼3 mm droplet diameter and different gap heights using 128° YX-LiNbO$_3$ SAW device with 1.5 mm aperture excited by a frequency of 60 MHz

(or droplet diameter, d), but also on the separation between the top plate and substrate (or gap height, H). Figure 2 shows the experimental results of the streaming velocities measured at the top centre of the droplets (point A as shown in Fig. 1) as a function of RF powers for different droplet volumes and gap heights. These results show that the streaming velocity increases with increase of the RF power, because at high powers, a higher acoustic pressure or momentum will be delivered to the liquid layer due to the increased SAW energy. A linear relationship between the streaming velocity and SAW power is observed for smaller gap heights such as of 271 and 102 μm in Fig. 2. This linearity is a reasonable, because of higher shear gradient of flow at the solid walls (e.g. top plate) with such small gap heights (Kamakura et al. 1995). This is in turn results in a slower flow motion in the droplet when Reynolds number value approaches unity. In this study, the droplet diameter, d, is used as the length scale in calculation of the Reynolds number. With such a small value of Reynolds number, inertial effects (hydrodynamics non-linearity) do not play a significant role in comparison with viscous effects, or creeping flow (Lighthill 1978). In contrast, a non-linear variation of streaming velocity with the RF power is obtained for a larger gap height of 548 μm. High speed camera observations revealed that the speed of polystyrene beads inside the droplets was only of 0.9 mm/s for a small gap height of 271 μm, whereas it was a 4.6 mm/s with larger gap height of 548, at the same RF power of ∼0.03 W. Results in Fig. 3 clearly show the influence of gap height on the SAW streaming flow.

Figure 3 shows the variation of streaming velocity data measured at point A, as shown in Fig. 1, as a function of

Fig. 3 Experimental results of streaming velocity at the *top* of droplet as a function of gap height for different power levels using 128° YX-LiNbO$_3$ SAW device with 1.5 mm aperture excited by a frequency of 60 MHz. **a** Droplet diameter of 3.0 mm; **b** droplet diameter of 2.2 mm
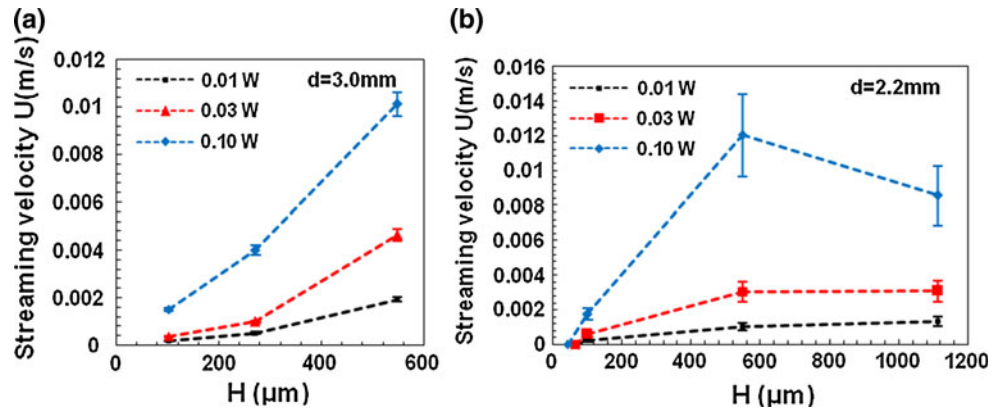
gap height, H, for droplets with nominal diameters of $\sim$2.2 and $\sim$3 mm, and SAW excitation powers of 0.01, 0.03 and 0.1 W. From results of $\sim$3 mm droplet diameters shown in Fig. 3a, the streaming velocity is suppressed as the gap height decreases, due to the increase in shear force gradient. Generally, the variation of streaming velocities with the gap height is nearly linear due to the lower value of inertial forces in comparison with viscous forces at lower velocities.

In general, the data in Fig. 3b for droplet with diameters of $\sim$2.2 mm show a similar phenomenon to those in Fig. 3a, where the streaming velocity is enhanced as the gap height increases. However, beyond a critical gap height of $\sim$550 μm, any further increase in the separation results in a decrease in the streaming velocity. As the acoustic energy loss is the only mechanism for the generation of acoustic streaming, and acoustic heating is also minimal at small applied power and fluid viscosity (Kondoh et al. 2005; Luong et al. 2011), this flow phenomenon can only be explained by the acoustic energy that was leaked into the liquid layer, a phenomenon which will be explained in details in Sect. 3.2.

Figure 4 shows numerical simulations of the detailed flow characteristics at various RF powers and gap heights. These results show that the streaming velocity (measured at point A in Fig. 1) increases with the gap height until reaching a critical value for the gap height, H_{cr}, of a 500 μm, above which the streaming velocity decreases. Considering the uncertainty associated with the experimental measurements, the critical value obtained from the simulation agrees well with the critical gap height of $\sim$550 μm obtained from the experimental measurements. However, when H is <500 μm, the streaming velocity decreases as the gap height decreases, which could be attributed to the increase in the dragging forces at the top and bottom solid boundaries (e.g. top glass plate) (Kang et al. 2005). With further reduction in the gap height to 50 μm, the simulated streaming velocity almost approaches zero, especially with RF powers <0.05 W.
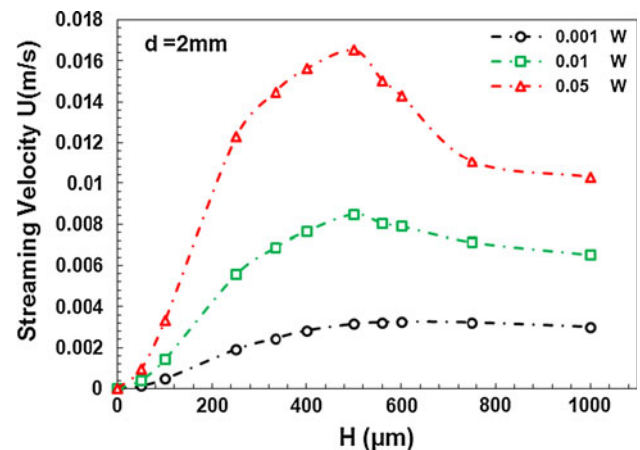

Fig. 4 Numerical results showing the maximum streaming velocity at the droplet centre as a function of gap height for 2 mm droplet diameter and different RF power levels, using 128° YX-LiNbO$_3$ SAW device with excitation frequency of 60 MHz

Indeed, our observations using a high speed camera showed that when the gap height was reduced to $\sim$65 μm, the velocity of polystyrene particles in the droplets was almost zero, and the liquid inside the droplet did not show any apparent flow patterns over the range of RF power used in this study, as can be observed in Fig. 3b. In general, the experimental results in Fig. 3 are in good agreement with those obtained from the numerical simulations shown in Fig. 4.

3.2 Physical mechanism

In order to explain the observed flow phenomena at various gap heights, the mechanism of SAW acoustic streaming and the SAW attenuation in the liquid layer should include a consideration of flow parameters, such as Reynolds number. A Rayleigh SAW can be generated by applying an alternating electric field to the IDT, as shown in Fig. 5a. The particles motion of Rayleigh SAW has two components, one is vertical and one is parallel to the surface

(Dransfeld and Salzmann 1970). If a liquid layer either in bulk or a droplet form lies in the propagation path of the emitted SAW, the normal component of SAW at the substrate surface causes an emission of longitudinal waves when it reaches the liquid layer. These waves propagate into the liquid at Rayleigh angle, as shown in Fig. 5a, because the velocity of longitudinal waves in the liquid layer, v_f, is much smaller than that of Rayleigh wave in substrate, v, as can be defined by $\sin \theta_R = v_f/v$ (Arzt et al. 1967). The emission of this compression (longitudinal) waves leads to an attenuation of SAW, within an absorption coefficient of α_l, which damps exponentially within an attenuation length of l_{SAW}, causing a change in its mode to a Leaky SAW (LSAW) (Shiokawa et al. 1989a, b), as shown in Fig. 5a. This damping length, l_{SAW}, of the SAW can be estimated using (Arzt et al. 1967; Dransfeld and Salzmann 1970; Schmid et al. 2011)

$$l_{SAW} = \frac{1}{\alpha_l} = \frac{\rho v \lambda}{\rho_f v_f} \qquad (1)$$

where λ is the wavelength of Rayleigh SAW, ρ_f and ρ is the density of the liquid and substrate material, respectively. In this study, a wavelength of $\lambda = 64$ μm and excitation frequency of $f = 60$ MHz were used, and the liquid (water) density is taken as $\rho_f = 1,000$ kg/m^3. The density of SAW device substrate (128° YX-LiNbO$_3$ material) is 4,630 kg/m^3 (Gantner et al. 2007). The calculated velocity of the SAW, v, is 3,840 m/s, based on $v = f\lambda$ (Berthier 2008), and the sound velocity in the liquid, v_f, is 1,500 m/s. It should be noted that the parallel component of the particle motion of Rayleigh

SAW at substrate surface leads to frictional losses, which can be calculated using the viscosity of liquid layer as

$$\alpha_S = \frac{\left(\rho_f \mu v^3/4\pi\right)^{1/2}}{\rho v^2} \qquad (2)$$

where α_s is the absorption coefficient of Rayleigh SAW due to viscous frictions and μ is the liquid viscosity (Arzt et al. 1967). The calculation based on Eqs. (1) and (2) shows that $\alpha_s \ll \alpha_l$. Therefore, in comparison with the contribution of longitudinal wave, the attenuation due to viscous losses can be neglected in this study (Shiokawa et al. 1989a, b).

Thus, the SAW attenuation length in this study was calculated using Eq. (1) with a value of $l_{SAW} \approx 750$ μm, i.e., a length required for the acoustic energy to be completely absorbed by the droplet liquid. The leakage of acoustic energy by SAW into the liquid droplet results in a net body force (force per unit volume), which can be written as (Shiokawa et al. 1990; Sankaranarayanan et al. 2008)

$$F = \rho_f(1 + \alpha_i^2)^{3/2} A^2 \omega^2 k_i \exp 2(k_i x + \alpha_i k_i y) \qquad (3)$$

where A represents the SAW amplitude at the interaction point between the SAW and liquid, and ω is angular frequency. k_L is the leaky SAW wave number which is a complex number $k_L = k_r + jk_i$, and can be calculated by applying the method of Campbell and Jones (1968, 1970) in the case of liquid–solid coupling. The imaginary part of the leaky SAW wave number computes the SAW energy dissipated into the fluid medium. The damping factor is $\alpha = j\alpha_i$ where $\alpha^2 = 1 - \left(\frac{v_L}{v_f}\right)^2$, and v_L is the velocity of leaky Rayleigh SAW (Shiokawa et al. 1990; Furukawa et al. 1991).

Fig. 5 Leaky SAW induces body force. a Illustration shows attenuation of leaky SAW by liquid coupling and the propagation direction of induced longitudinal wave; b calculated streaming force at SAW interaction point and along the propagation direction of the longitudinal wave towards the upper glass slide
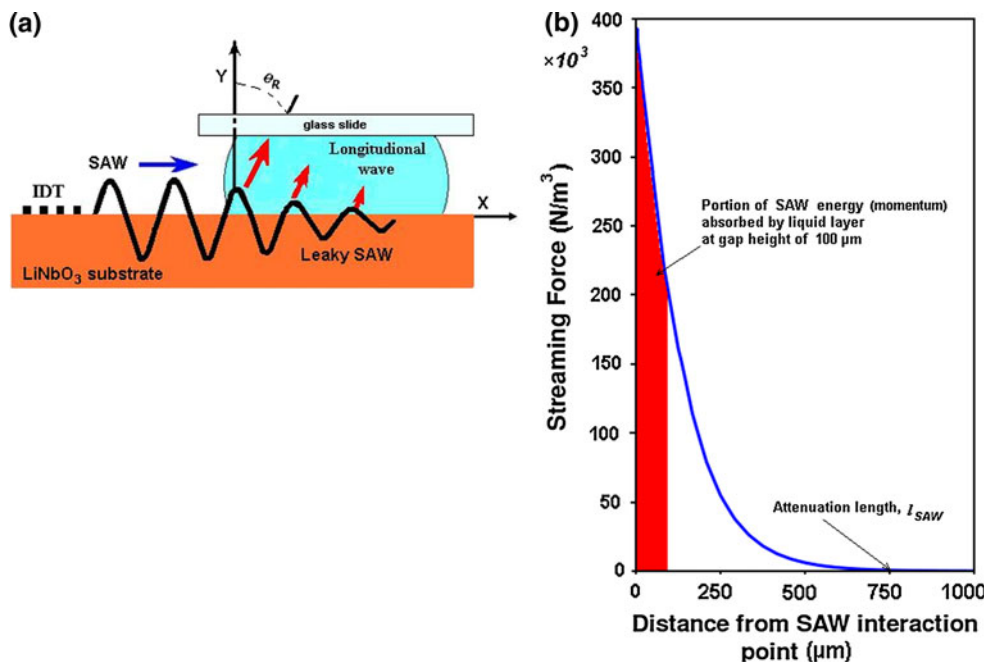
Both the experimental and numerical results show that, when the gap height is less than ~ 500 μm, the streaming velocity is enhanced with increasing gap height. In this regime, the acoustic energy absorbed by the liquid layer due to the emission of longitudinal waves induces an acoustic streaming flow. If these waves propagate through a liquid layer of gap heights less than its damping length, a part of the longitudinal waves will be refracted from the liquid layer into the upper glass slide, which means that less energy will be coupled into the liquid layer. Indeed, the distribution profile of streaming force presented in Fig. 5b shows that the portion of acoustic momentum delivered to the liquid by the SAW per unit area (area under curve) at small gap heights such as 100 μm is smaller than that of larger heights. Therefore, with a smaller gap, less energy will be delivered from the SAW. Also the corresponding increase in the wall shear resistance from the top plate will contribute to a decrease in the streaming velocity. Therefore, any increase in the gap height will enhance the SAW momentum, and hence the streaming velocity.

However, it has been shown earlier in this paper that if the gap height is increased beyond a critical value of ~ 500 μm, the streaming velocity will drop gradually, as shown in Figs. 3 and 4. This reduction in the value of streaming velocity with gap heights larger than ~ 500 μm can also be explained from Fig. 5b. An increase in the gap height beyond a 500 μm will induce a negligible improve in the SAW momentum delivered to the fluid, where the most of the acoustic momentum is already coupled into the fluid. On the other hand, there is a large increase in the mass inertia of the droplet volume with increased gap height, which could explain the decrease of the streaming velocities as the gap heights larger than ~ 500 μm.

Figure 6 shows simulation results of Reynolds number (using the value of the streaming velocity at point A, shown in Fig. 1) as a function of the normalized gap height, H/l_{SAW}, for a range of acoustic powers (the droplet diameter is 2 mm). This reveals that if the gap height, H, exceeds a critical percent of the attenuation length of Rayleigh SAW l_{SAW}, which has been identified as $\left(\frac{H}{l_{SAW}}\right)_{cr} \approx 0.7$, the Reynolds number decreases dramatically with further increases in the gap height, especially at excitation powers larger than 1 mW, which corresponds to a critical gap height of $H_{cr} \approx 500$ μm, in which the amplitude of the LSAW nearly attenuates to $\sim 1/e$, as shown by the value of streaming force in Fig. 5b.

For smaller gap heights, as the dimensionless gap height ratio, H/l_{SAW} is <0.067 (equivalent to $H < 50$ μm), the momentum of the SAW produces a slower flow motion (with $Re \leq 1$) even at the highest power of 0.05 W in this study (see Fig. 6). From experiments, the motion of polystyrene particles becomes undetectable when gap
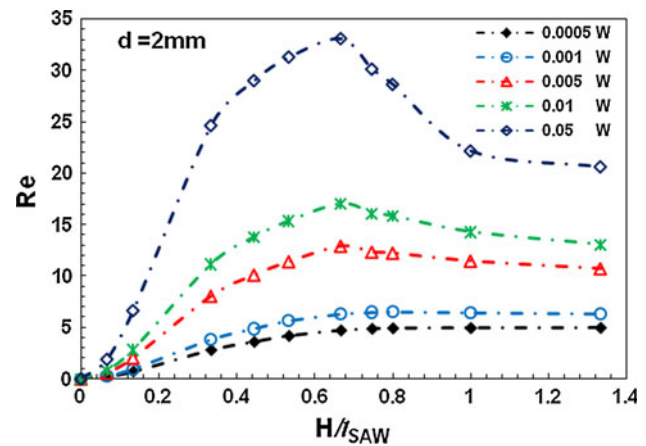

Fig. 6 Numerical results of Reynolds number as a function of normalized gap height for 2 mm droplet diameter excited by a range of powers using 128° YX-LiNbO$_3$ SAW device with 1.5 mm aperture and excitation frequency of 60 MHz

heights are <100 μm, and the polystyrene particles quickly adhered to substrate surface due to the large shear gradients generated near the solid surfaces at small gap heights (Zeng et al. 2011), as shown in Fig. 6. During the experiments with gap height of 65 μm, there was no apparent streaming effect or motion of the polystyrene particles even when the applied RF power was increased up to 20 W. However, these higher powers induce a significant heating effect, causing the severe evaporation of the liquid as shown in Fig. 7. Weilin et al. (2000) have also reported a similar significant increase in the viscous friction in the case of liquid flows in trapezoidal silicon microchannel when the channel height was changed from 111 to 28 μm.

Figure 8 shows the simulated streaming velocity profiles as a function of distance above the substrate for a range of gap heights and RF powers measured at the droplet centre through its height. Figure 9 shows the corresponding velocity vectors values at a gap height of 1,000 μm and measured at centre of the droplet through its height. Figure 8a shows that when the gap height exceeds 500 μm at an excitation RF power of 5 mW, there is a gradual decrease in the streaming velocity. Below this value, the velocity also reduces and when the gap height is <100 μm, the streaming velocity decreases to <20 % of the peak value. For gap heights of 50 μm, the induced streaming is actually a creeping motion with a very low Reynolds number of $Re \leq 1$. Figure 8b shows results for an RF power of 100 mW, and similarly the streaming velocity is strongly suppressed as long as the gap height is <100 μm (or $H/l_{SAW} < 0.13$), with a minor difference in velocity profiles for a gap height of 1,000 μm compared with Fig. 8a. This is mainly due to the significant increase in velocity at the top of droplet, resulting from increasing the RF power from 5 to 100 mW. These can be clearly

Fig. 7 Experimental captured images of a droplet located on a 128° YX-LiNbO$_3$ substrate in line with a SAW device with 1.5 mm aperture and gap height of 65 μm (*top view*). **a** Before applying the RF power; **b** after application of 20 W RF power and excitation frequency of 60 MHz, showing the heating and evaporation
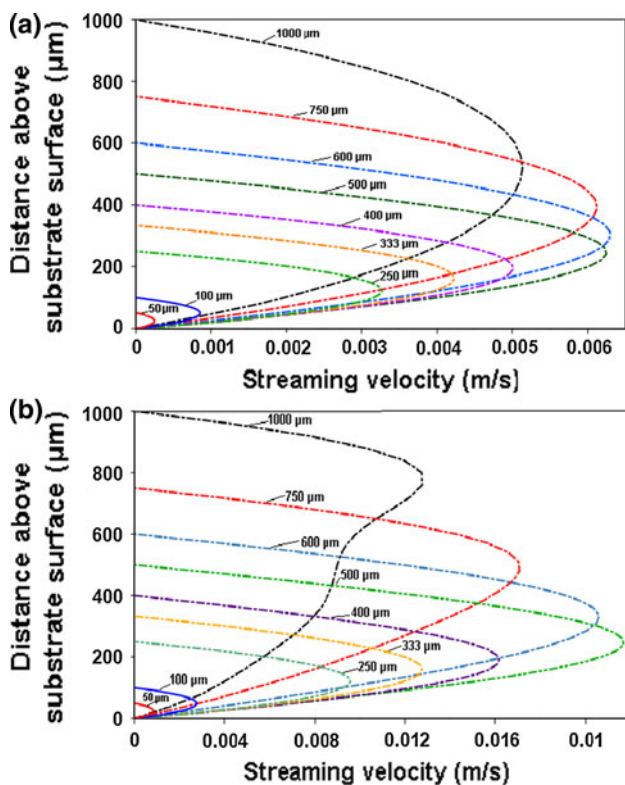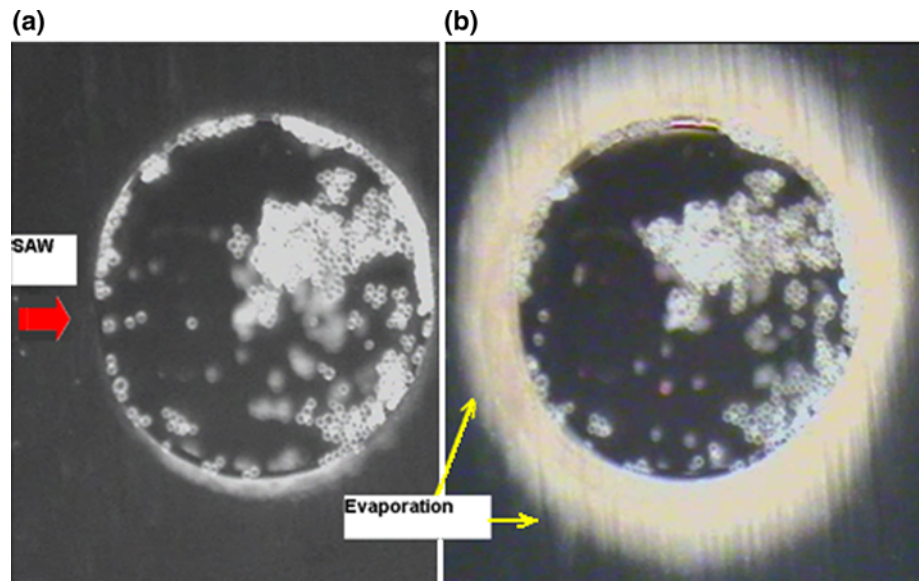

Fig. 8 Numerical simulation results of the velocity profile for a 2 mm droplet diameter with different gap heights and measured at the droplet centre through its height; using 128° YX-LiNbO$_3$ SAW device with 1.5 mm aperture excited by a frequency of 60 MHz; **a** at RF power 5 mW; **b** at RF power 100 mW
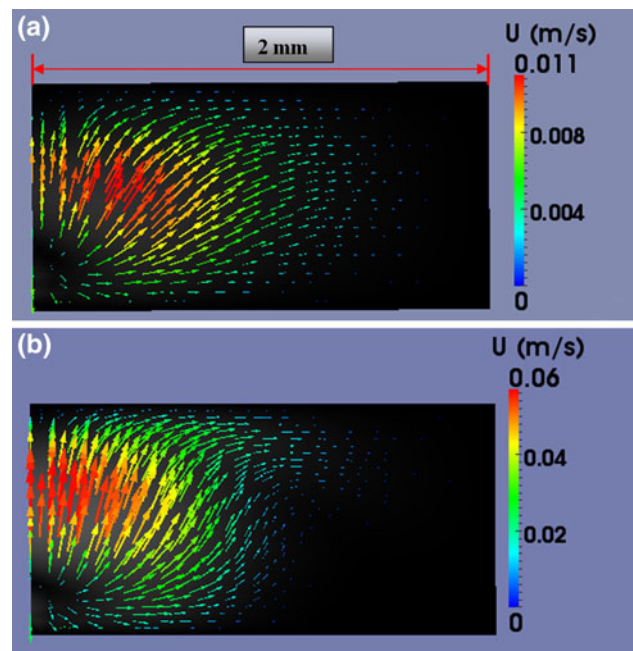

Fig. 9 Cross-sectional numerical simulation results of velocity vectors values of 2 mm droplet at gap height of 1,000 μm and measured at centre of the droplet through its height; using 128° YX-LiNbO$_3$ SAW device excited by a frequency of 60 MHz; **a** at RF power 5 mW; **b** at RF power of 100 mW. *Coloured vectors* show flow direction and velocity value

revealed from the differences in the velocity vectors illustrated in Fig. 9 for the two different SAW powers. Besides, the results in Fig. 3b show that the flow symmetry along the gap height is broken (e.g. asymmetry velocity profile) for gap heights beyond H_{cr}, of a 500 μm.

4 Conclusion

This study presents an experimental and numerical investigation for the scaling effects on the characteristic flow hydrodynamics in a confined microdroplet induced by SAW. The configuration of the study set-up includes a top glass slide and LiNbO$_3$ substrate on the propagation path of a SAW, between which a liquid microdroplet was placed.

The microfluidic experiments were carried out using 128°
YX-LiNbO$_3$ SAW devices excited with a frequency of
60 MHz. Analysis from both the experimental and
numerical results showed that, compared with freestanding
droplets, there is a significant scaling effect that influences
the streaming behavior of flow hydrodynamics in the
microdroplets confined between the two plates. For
example, if the gap height, H, is <100 μm, the character-
istic streaming velocity reduces considerably with a
decrease in the gap height, and approaches zero at a gap
height of 50 μm. Therefore, the ability of using the SAW
momentum to drive the fluids into confined spaces or mi-
crochannels at smaller gap heights will be problematic, due
to the increased wall shear gradient at smaller gap heights
(Zeng et al. 2011). Furthermore, it has been observed that
there is a critical value for the gap height, above which the
streaming velocity decreases. This critical value have been
characterised by a dimensionless ratio of the gap height,
H, and the attenuation length of the Rayleigh SAW, where
the detailed experimental and numerical results have
revealed this critical value to be $\left(\frac{H}{l_{\text{SAW}}}\right)_{\text{cr}} \approx 0.7$.

References

Alghane M, Chen BX et al (2010) Experimental and numerical
    investigation of acoustic streaming excited by using a surface
    acoustic wave device on a 128° YX-LiNbO3 substrate. J Micro-
    mech Microeng 21:015005

Alghane M, Fu YQ et al (2011) Streaming phenomena in microdro-
    plets induced by Rayleigh surface acoustic wave. J Appl Phys
    109:114901

Arzt RM, Salzmann E et al (1967) Elastic surface waves in quartz at
    316 MHz. Appl Phys Lett 10(5):165–167

Berthier J (2008) Microdrops and digital microfluidic. William
    Andrew Inc, Norwich

Campbell JC, Jones WR (1968) A method for estimating optimal
    crystal cuts and propagation direction for excitation of piezo-
    electric surface waves. IEEE Trans Sonic Ultrasonics 15:209

Campbell JC, Jones WR (1970) Propagation of surface waves at the
    boundary between a piezoelectric crystal and a fluid medium.
    IEEE Trans Sonic Ultrasonics 17:71–76

Dransfeld K, Salzmann E (1970) Excitation, detection and attenuation
    of high-frequency elastic surface waves. In: Mason WP, Thurston
    RN (eds) Physical acoustics. Academic press, New York,
    pp 219–272

Franke TA, Wixforth A (2008) Microfluidics for miniaturized
    laboratories on a chip. Chem Phys Chem 9:2140–2156

Friend J, Yeo LY (2011) Microscale acoustofluidics: microfluidics
    driven via acoustics and ultrasonics. Rev Mod Phys 83(2):647–
    704

Frommelt T, Gogel TD et al (2008a) Flow patterns and transport in
    Rayleigh surface acoustic wave streaming. IEEE Trans Ultra-
    sonics 55:2298–2305

Frommelt T, Kostur M et al (2008b) Microfluidic mixing via acousti-
    cally driven chaotic advection. Phys Rev Lett 100(3):034502

Furukawa S, Nomura T et al (1991) Characteristic features of leaky
    surface acoustic waves propagating on liquid/piezoelectric film
    glass structures. J Phys D Appl Phys 24(5):706–713

Gantner A, Hoppe RHW et al (2007) Numerical simulation of
    piezoelectrically agitated surface acoustic waves on microfluidic
    biochips. Comput Vis Sci 10(3):145–161

Guo H, Sun H et al (2008) Theoretical study of acoustic streaming
    induced cooling effect in the microscale. In: Proceedings of
    IEEE International Ultrasonics Symposium, pp 934–937

Gu H-h, Zhang S-y et al (2009) Study on non-contact linear motors
    driven by surface acoustic waves. Sens Actuators A 155:163–
    167

Kamakura T, Matsuda K et al (1995) Acoustic streaming induced in
    focused Gaussian beams. J Acoust Soc Am 97(5):2740–2746

Kang K, Lee LJ et al (2005) High shear microfluidics and its
    application in rheological measurement. Exp Fluids 38(2):222–
    232

Kondoh J, Shimizu N et al (2005) Temperature-control system for
    small droplet using surface acoustic wave device. Sensors, 2005
    IEEE

Lighthill J (1978) Internal waves in fluids. Cambridge University
    Press, Cambridge

Luong T-D, Phan V-N et al (2011) High-throughput micromixers
    based on acoustic streaming induced by surface acoustic wave.
    Microfluid Nanofluid 10(3):619–625

Min-Chien T, Tzong-Shyng L (2007) The study of flexible plate wave
    device for micro pumping system. In: 2nd IEEE International
    Conference, Nano/Micro Engineered and Molecular Systems,
    2007 (NEMS '07)

Nam-Trung N, White RM (2000) Acoustic streaming in microma-
    chined flexural plate wave devices: numerical simulation and
    experimental verification. Ultrasonics, Ferroelectrics and Fre-
    quency Control. IEEE Trans 47(6):1463–1471

Nguyen NT, White RM (1999) Design and optimization of an
    ultrasonic flexural plate wave micropump using numerical
    simulation. Sens Actuators A 77(3):229–236

Patankar SV (1980) Numerical heat transfer and fluid flow. Hemi-
    sphere Publishing Corporation, New York

Sankaranarayanan SKRS, Cular S et al (2008) Flow induced by
    acoustic streaming on surface-acoustic-wave devices and its
    application in biofouling removal: a computational study and
    comparisons to experiment. Phys Rev E 77(6):066308

Schmid L, Wixforth A et al (2011) Novel surface acoustic wave
    (SAW)-driven closed PDMS flow chamber. Microfluid Nano-
    fluid 12:1–7

Shiokawa S, Matsui Y et al (1989a) Liquid streaming and droplet
    formation caused by leaky Rayleigh waves. In: Proceedings of
    IEEE Ultrasonics Symposium, 1989

Shiokawa S, Matsui Y et al (1989b) Experimental study on liquid
    streaming by SAW. Jpn J Appl Phys 28(Suppl 28-1):126–128

Shiokawa S, Matsui Y et al (1990) Study on acoustic streaming and
    its application to fluid devices. Jpn J Appl Phys 29:137–139

Tan M, Friend J et al (2007) Surface acoustic wave driven
    microchannel flow. In: Proceedings of 16th Australasian Fluid
    Mech Conference, Gold Coast, Australia

Tan MK, Yeo LL et al (2009) Inducing rapid fluid flows in
    microchannels with surface acoustic waves. In: IEEE Interna-
    tional Ultrasonics Symposium (IUS)

Tan MK, Yeo LY et al (2010) Unique flow transitions and particle collection switching phenomena in a microchannel induced by surface acoustic waves. Appl Phys Lett 97(23): 234106-3

Tzong-Shyng L, Horng-Jiann S (2009) New pumping mechanism by surface waves in a microchannel. In: 4th IEEE International Conference on Nano/Micro Engineered and Molecular Systems, 2009 (NEMS 2009)

Weilin Q, Mohiuddin Mala G et al (2000) Pressure-driven water flows in trapezoidal silicon microchannels. Int J Heat Mass Transf 43(3):353–364

Wixforth A (2003) Acoustically driven planar microfluidics. Superlattices Microstruct 33:389–396

Zeng Q, Guo F et al (2011) Milliseconds mixing in microfluidic channel using focused surface acoustic wave. Sens Actuators B Chem 160(1):1552–1556